PCCP

Accepted Manuscript

ROYAL SOCIETY OF CHEMISTRY

www.rsc.org/pccp

On the origin of the substantial stabilisation of the electron-donor 1,3-dithiole-2-thione-4-carboxyclic acid...I_2 and DABCO...I_2 complexes

Palanisamy Deepa,[1] Robert Sedlak[1] and Pavel Hobza*[1,2]

[1]Institute of Organic Chemistry and Biochemistry, Academy of Sciences of the Czech Republic, Flemingovo nám. 2, 166 10 Prague 6, Czech Republic

E-mail: *pavel.hobza@uochb.cas.cz*

[2]Regional Centre of Advanced Technologies and Materials, Department of Physical Chemistry, Palacky University, 771 46 Olomouc, Czech Republic

Abstract

The stabilisation energies of the crystal structures of 1,3-dithiole-2-thione-4-carboxyclic acid...I_2 and DABCO...I_2 complexes determined by the CCSD(T)/CBS method are very large and exceed 8 and 15 kcal/mol, respectively. The DFT-D method (B97-D3/def2-QZVP) strongly overestimates these stabilisation energies, which supports the well-known fact that the DFT-D method is not very applicable for the study of charge-transfer complexes. On the other hand, the M06-2X/def2-QZVP method provides surprisingly reliable energies. A DFT-SAPT analysis has shown that a substantial stabilisation of these complexes arises from the charge-transfer energy included in the induction energy and that the respective induction energy is much larger than that of other non-covalently bound complexes. The total stabilisation energies of the complexes mentioned as well as of those where iodine has been replaced by lighter halogens (Br_2 and Cl_2) or by hetero systems (IF, ICH_3, N_2) correlates well with the magnitude of the σ-hole ($V_{s,max}$ value) as well as with the LUMO energy. The nature of the stabilisation of all complexes between both electron donors and X_2 (X=I, Br, Cl, N) systems is explained by the magnitude of the σ-hole but surprisingly also by the values of the electric quadrupole moment of these systems. Evidently, the nature of the stabilisation of halogen-bonded complexes between electron donors and systems where the first nonzero electric multipole moment is the quadrupole moment can be explained by the recently introduced concept of the σ-hole but also by the classical concept of electric quadrupole moments.

Introduction

Complexes containing halogens participating in halogen bonding (X-bonding) are characterised by large stability, mostly comparable with the stabilisation of similar H-bonded complexes. Indeed, accurate CCSD(T)/CBS stabilisation energies of complexes with halogens (X40 data set[1]) and H-bonded complexes from the S66 dataset[2,3] are well comparable. In both cases, energy decomposition is similar, with electrostatic energy playing a dominant role. A counterintuitive electrostatic attraction in the case of a X-Y...D halogen bond, where Y is Cl, Br or I, X is an electronegative atom (mostly carbon) and D is an electron donor like oxygen, nitrogen or sulpur, is explained by the existence of a positive σ-hole on top of the halogen atom[4-6]. The electrostatic attraction thus occurs between the positive σ-hole and a negative electron donor. In the case of an X-H...D hydrogen bond,[7,8] the electronegative attraction is caused by the interaction between a positively charged hydrogen and a negatively charged electron donor. A comparison of other energy contributions reveals that dispersion energy is more negative in X-bonds than in H-bonds, which is explained by the fact that halogen and electron donors, both having large polarisability, are close each to other. The last attractive energy, induction energy, is mostly smaller than dispersion energy; in X- and H-bonds, it is comparable. Induction energy in a broader sense of the SAPT[9-17] contains, apart from exchange induction, also the δHF term, which covers higher-order terms. The induction energy thus contains not only classical multiple-induced multiple induction energy but also charge-transfer energy. The charge-transfer energy becomes important only if an electron donor effectively interacts with an electron acceptor. This means that besides the highest-occupied molecular orbital (HOMO) of the donor and the lowest-unoccupied molecular orbital (LUMO) of the acceptor, there must also be a favourable overlap between these orbitals.

In our recent study,[18] we investigated the crystal structures containing iodine; among them, we found one structure (1,3-dithiole-2-thione-4-carboxyclic acid (DTCA)...I_2), for which we obtained a surprisingly large stabilisation energy exceeding 10 kcal/mol. Then we searched in the literature[19] and found a similar complex (DABCO...I_2) with an even larger stabilisation energy close to 20 kcal/mol. Since both calculations were made at a lower theoretical level, it is not clear whether these surprising numbers are correct. If they are, where does this large stabilisation come from? Is it only caused by halogen bonding with heavy iodine or does charge transfer play an important role here?

The aim of the present study is to investigate in detail the nature of the interactions in the above-mentioned complexes. To elucidate the role of I_2, we will also study complexes where I_2 is replaced by lighter halogens (Br_2, Cl_2), hetero dihalogen (IF) as well as other systems (ICH_3, N_2). The benchmark stabilisation energies will be evaluated at the CCSD(T)/CBS level[1,2] and the energy components will be obtained from SAPT calculations.[20]

Calculations

The electrostatic potentials have been computed on molecular surfaces, with a surface being defined as the 0.001 a.u. (electrons/bohr^3) outer contour of the electron density, as proposed by Bader et al.[21] The most positive value of the potentials at the halogen (the local maximum) is referred to as $V_{s,\,max}$. Here, the electrostatic potentials as well as the geometries of electron acceptors and their electric quadrupole moments were calculated at the B97-D3/def2-QZVP level.[22-24]

The benchmark stabilisation energies were evaluated using the CCSD(T)/CBS method. Specifically, these stabilisation energies were constructed as the sum of the HF/CBS and MP2/CBS interaction energy. Both CBS energies were obtained via 2 point Helgaker

extrapolation from aug-cc-pVDZ and aug-cc-pVTZ basis sets.[25,26] The CCSD(T) correction term ($\Delta E^{CCSD(T)} - \Delta E^{MP2}$) was evaluated with an aug-cc-pVDZ basis set. The theoretical level used for benchmark calculation represents a compromise between accuracy and economy. A more detailed description of present procedure can be found in our previous paper.[1,2] The M06-2X functional was recommended[27] for calculations of halogen-bonded complexes and it was also used in the present study. Besides DFT-D (B97-D3/def2-QZVP), also M06-2X/ def2-QZVP calculations[28] were performed. All interaction energies calculations were corrected for the basis set superposition error (BSSE) utilizing counterpoise correction.[29]

Energy decomposition of the stabilisation energies of all complexes was obtained by using the DFT-SAPT method.[9-17] The DFT part was treated using asymptotically corrected the PBE0AC exchange-correlation functional and an aug-cc-pVDZ basis set. The total interaction energy in the DFT-SAPT is given as the sum of the first- (E_1) and second-order (E_2) perturbation energy terms and δHF energy terms, specifically electrostatic (E_1^{Pol}), induction (E_2^{ind}) and dispersion (E_2^{disp}) energy terms together with exchange-repulsion terms (E_1^{Ex}, $E_2^{ex\text{-}ind}$ and $E_2^{ex\text{-}disp}$). The exchange-induction and exchange-dispersion terms are merged into the respective induction (E_2^{Ind}) and dispersion terms (E_2^{Disp}); furthermore, the δHF term, which represents higher than second-order electrostatic and induction terms covered by the Hartree-Fock approach, was calculated separately, utilizing aug-cc-pVDZ basis set. The δHF term is defined as a difference between the HF stabilization energy and sum of E_1^{Pol}, E_1^{Exch}, E_2^{ind} and $E_2^{ex\text{-}ind}$ energies calculated at the HF-SAPT level. The δHF term is also included in the induction energy (E_2^{Ind}).

$$E_{int}=E_1^{Pol}+E_1^{Ex}+E_2^{ind}+E_2^{ex\text{-}ind}+E_2^{disp}+E_2^{ex\text{-}disp}+\delta HF=E_1^{Pol}+E_1^{Ex}+E_2^{Ind}+E_2^{Disp} \quad (1)$$

The greatest improvement of the DFT-SAPT method over the original SAPT is the acceleration of the calculations by one order of magnitude[9-17]. The intramolecular treatment is conducted using the DFT and therefore suffers from inaccurate energies of the virtual

orbitals. This drawback is corrected before the actual SAPT treatment by a gradient-controlled shift procedure, which uses the difference between the exact vertical ionisation potential (IP) and the energy of the (HOMO).[13] In this work, PBE0/aug-cc-pVTZ and PBE0/aug-cc-pVDZ calculations were carried out to obtain the IP respective HOMO values.

All the post Hartree-Fock calculations (including DFT-SAPT) were carried out using the Molpro 2010 package.[30] The DFT based methods, excluding M062X, were done utilizing the Turbomole 6.3 package.[31] The M062X calculations were carried out using Gaussian 09 package.[32]

Structures

The coordinates of heavy atoms for both the I_2 complexes were taken from X-ray structures.[18-19] Afterwards, hydrogen atoms were manually added using Molden program[33] and subsequently optimized at the B97-D3/def2-QZVP level of theory, while keeping the coordinates of the heavy atoms frozen (cf. Fig. 1).

When constructing the geometries of other binary complexes, the following procedure was utilized. Firstly, the coordinates of the DTCA and DABCO molecule were taken from structures of respective I_2 complexes. Secondly, when I_2 molecule was replaced from the corresponding I_2 complex structure by X_2 (X=Br, Cl, N) or XY (Y=F, CH_3) systems, the closer halogen atom X_1 coincides with closer iodine atom (cf. Fig. 1). Finally, the rest of the electron acceptor molecule was constructed using the optimized geometry of the isolated acceptor, which was calculated at the B97-D3/def2-QZVP level of theory (cf. Fig. 1).

Results and Discussion

Isolated systems

The geometries of all electron donors as well as electron acceptors taken from X-ray crystal structures or optimised are collected in Table S1 of the Supporting Information.

The LUMO energies of the acceptors are summarised in Table 1, which also contains the $V_{s,max}$ values and the quadrupole moment for all electron acceptors. The electrostatic potentials for selected monomers are visualised in Fig. 2.

Investigating the LUMO values, we find that IF, I_2 and Br_2 are the best acceptors. The Cl_2 systems are slightly worse and the N_2 molecule has the LUMO at higher energies, which agrees with the fact that N_2 is not an electron acceptor. The same is true for ICH_3 systems. The HOMO values for the electron donors DTCA and DABCO is -0.199 and -0.144 a. u., respectively; this means that the DABCO is a better electron donor.

As expected, the magnitude of the σ-hole (see the $V_{s,max}$ value) for I_2 is larger than that of Br_2 and Cl_2. When the iodine was replaced by the more electronegative fluorine, the $V_{s,max}$ value increased considerably. The $V_{s,max}$ for N_2 is negative, which provides evidence that the positive σ-hole does not exist here. Comparing the quadrupoles of X_2 molecules, we find that they have different signs for halogens (I_2, Br_2, Cl_2) and the nitrogen. The quadrupoles of the halogens can thus be schematically written as + - - + while that of the nitrogen as - + + -. Evidently, the schematic notations reflect the concept of the σ-hole. The correlation between the $V_{s,max}$ and the quadrupole moment for the X_2 systems is shown in Fig. 3a and, evidently, it is very high (R^2=0.902). This finding is surprising, because it tells us that for the explanation of the different binding of the halogens (Cl_2, Br_2, I_2) and the nitrogen to electron donors like O or N, it is not necessary to introduce a concept of the σ-hole, but it is enough to consider classical quadrupole moments. The electron donors with halogens exhibit attraction while the electron donors with nitrogen repulsion. This can be easily explained by the values of $V_{s,max}$ but comparably easily by quadrupole moments. Clearly, this is valid only for the X_2 systems where the first non-vanishing electric multipole moment is quadrupole. In the case of XY systems such IF, the first non-vanishing electric multipole

moment is the dipole moment and here the bonding of this system to an electron donor can only be explained by using the σ-hole.

Complexes

Table 2 contains interaction energies determined for all complexes investigated using various computational techniques. The B97-D3 stabilization energies for the complexes with halogens are very large; for DABCO complexes, they are even 40–70 % larger. The larger stabilisation of the DABCO complexes can be easily explained by the fact that DABCO is a better electron acceptor (see above). In both complexes, dispersion energy (shown in Table 2, 1st column in parentheses) is an important stabilisation component, but it is not dominant. For further energy decomposition, see the SAPT calculations. As mentioned in the Introduction, the DFT stabilisation energies for the charge-transfer complexes could be overestimated due to an unrealistic description of the virtual space. The benchmark stabilisation energies are produced by the CCSD(T)/CBS calculations, as seen from Table 2, these energies are considerably smaller than the DFT ones. Considering all the complexes with attractive interaction, we found that the CCSD(T)/CBS stabilisation energy forms on average 62 % of the DFT-D stabilisation energy for the DTCA complexes and 79 % for the DABCO complexes. The CCSD(T)/CBS stabilisation energies of the DABCO complexes are larger than those of the DTCA complexes (by 11–139 %). Surprisingly accurate numbers are obtained with the M06-2X functional and the respective correlations (R^2 = 0.983, R^2=0.994) between the M06-2X and the CCSD(T)/CBS energies for both complexes are shown in Fig. 3b. The MP2/CBS stabilization energies are systematically overestimated with respect to CCSD(T)/CBS values. The average overestimation for the DABCO and the DTCA complexes evaluates to 32% and 37 %, respectively. The DFT-SAPT calculations provide stabilisation energies smaller than the benchmark CCSD(T)/CBS values, but the correlation

between both energies is quite close (R^2 =0.990, R^2 =0.923, see Fig. 3c). The underestimation of the SAPT energies arises from the use of a small aug-cc-pVDZ basis set. Among various energies, dispersion energy is the most underestimated.[14] We, however, use the SAPT not for generating accurate total stabilisation energies but for a mere decomposition of the total stabilisation energies.

Passing from iodine to chlorine, the stabilisation energies of both complexes decrease, the drop between iodine and bromine is moderate, but it becomes larger between bromine and chlorine. The stabilisation energies of chlorine complexes are considerably smaller than those of iodine complexes, but they are still substantial. A dramatic increase of the stabilisation energies of both complexes occurs when I_2 is replaced (at the same geometry) by IF. The electronegative fluorine withdraws electrons from iodine, which results in a much larger magnitude of the σ-hole (see Table 1 and Fig. 2). Consequently, also the total stabilisation energies increase. On the other hand, when one iodine atom in the iodine molecule is replaced by an electron-pushing CH_3 group, the $V_{s,max}$ decreases and the total stabilisation energy decreases dramatically and even becomes repulsive. Very large stabilisation energies of complexes with IF are also caused the fact that this molecule is the best electron acceptor among all of the systems investigated (see Table 1). The replacement of an iodine molecule with a nitrogen molecule also results in larger repulsive interaction energy. Here again, a certain role is played by both effects (nitrogen is not a good electron acceptor and does not contain a positive σ-hole). These findings indicate that electrostatic and charge-transfer energies play an important role in the complexes investigated.

To understand the nature of the stabilisation of both complexes, we performed a SAPT decomposition, and the single-energy terms are shown in Table 3. From the Table 3, it becomes clear that SAPT energies are determined as a sum of differently large numbers. The largest energy (in the absolute value) is exchange-repulsion energy E_1^{Exch}, which indicates

short intermolecular distances. Indeed, this finding is supported by the intermolecular distances shown in Fig. 1. Among attractive terms, the largest energy is electrostatic energy E_1^{Pol}. In both complexes, dispersion energy E_2^{Disp} is large but induction energy E_2^{Ind} (the sum of induction, exchange-induction and δHF energies) is comparable or in some cases even larger. This is clearly a new phenomenon in all of our previous studies[34-59] on noncovalent complexes including X-bonded complexes, the induction energy was systematically the smallest attractive term.

In this paragraph we will discuss the magnitude of the dispersion interaction, electrostatic and induction will follow in next. Comparing the value of E_2^{Disp} from DFT-SAPT, and D3 from B97-D3 (cf. Table 2) it is obvious that E_2^{Disp} term is in systematically more negative. The E_2^{Disp} term is larger (in absolute value) in average by 94 % and 73 % for DTCA and DABCO complexes, respectively. This is in contrast with magnitudes of whole stabilization energies (as discussed above). This counterintuitive result can be understood as a consequence of the vagueness, when define the dispersion interaction within framework of the DFT. The Grimme's empirical correction to dispersion interaction (D3) is trying to remove one of the most important drawbacks of the exchange-correlation functional in DFT, which is inability to reproduce dispersion interaction, but not only at asymptotic region ($1/R^6$ dependence) but in whole range of distances. However, we should keep in mind that "local" or "semi-local" functional, such as B97, can cover some part of dispersion interaction. When describing the medium-range attractive noncovalent interaction at the van der Waals distances, where intermolecular overlap is not negligible. Hence, we stress that the Grimme's D3 correction represent only part of dispersion. On the other hand, E_2^{Disp} term from DFT-SAPT, which is based on second order perturbation theory, represents better approximation to exact dispersion. That is why, the E_2^{Disp} term covers bigger portion of dispersion (i.e. is more negative) than empirical D3 correction. Finally, we would like to point out that presented

difference between the E_2^{Disp} term and D3 dispersion correction is underestimated. This follows from the fact that aug-cc-pVDZ basis set do not provide sufficiently converged value of the E_2^{Disp} term. This term is underestimated roughly by 10-20 %, at this level.[14]

Now we will try to explain the magnitude of electrostatic and induction energies. First, we will investigate the correlation between electrostatic energy and the values of $V_{s,max}$ on the one hand and the quadrupole moment of X_2 molecules on the other. Evidently, both correlations (DTCA: 0.635, 0.894; DABCO 0.673, 0.917; Figs. 3d, 3e) are high, showing again that the σ-hole as well as the quadrupole moment explain significant electrostatic stabilisation in X-bonded complexes. When going from X_2 molecules to other electron acceptors (IF, ICH_3) for which the first non-zero multipole moment is the dipole moment, the concept of quadrupole moment cannot be used any more. The correlation between electrostatic energy and $V_{s,max}$ for all six electron acceptors and both electron donors is, however, not very high (DTCA 0.404; DABCO 0.441; Fig. 3f) and it is slightly better for the correlations between induction energy and $V_{s,max}$ (DTCA 0.815, DABCO 0.795; Fig. 3g). Evidently, electrostatic as well as induction energies depend on more variables than only on the magnitude of the σ-hole. As mentioned above, induction energy contains a charge-transfer term which depends on the ability of an electron donor to donate electrons and an electron acceptor to accept electrons. The correlations between the induction energy and the LUMO energy of the electron acceptors for DTCA and DABCO are comparable (0.756 and 0.593; Fig. 3h). This tells us that charge-transfer energy plays a dominant role in induction energy. We have seen above that the $V_{s,max}$ value does not correlate tightly with neither electrostatic nor induction energies. However, the correlation between the SAPT interaction energy and the $V_{s,max}$ value (0.873 and 0.910; Fig. 3i) as well as between the CCSD(T)/CBS interaction energy and the $V_{s,max}$ value (0.932 and 0.950; Fig. 3j) is much higher. Little worse correlation has been found between the SAPT interaction energy and the LUMO energy of

the acceptor (0.787 and 0.688; Fig. 3k) and the CCSD(T)/CBS interaction energy and LUMO energy of the acceptor (0.782 and 0.873; Fig. 3l). It is thus possible to conclude that the $V_{s,max}$ value as well as the LUMO energy of the electron acceptor provide almost complete information on the stabilisation of the complexes investigated.

We should further investigate the composition of the total SAPT interaction energy. The SAPT energy correlates best with the total induction energy (0.953 and 0.935; Fig. 3m), whereas the correlation with electrostatic and dispersion energy is considerably worse. Putting together this and previous conclusions, we can state that within all of the complexes investigated, the charge-transfer energy included in the SAPT induction energy represents the most important energy term. Among the single characteristics of the acceptor, the $V_{s,max}$ value as well as LUMO energy of the acceptor correlate best with the total interaction energies.

Conclusions

i) The CCSD(T)/CBS stabilisation energies of the DTCA...I_2 and DABCO...I_2 charge-transfer complexes are very large, exceeding 8 and 15 kcal/mol, respectively. The B97-D3/def2-QZVP stabilisation energies of these complexes are strongly overestimated while the M062X/def2-QZVP energies agree with the benchmark values very well. DFT-SAPT stabilisation energies are smaller than the benchmark values, which arises from the use of aug-cc-pVDZ basis set which underestimate dispersion interaction.

ii) The stabilisation energies of both complexes decrease when passing from iodine to chlorine and dramatically increase when iodine with IF. When replacing halogen electron acceptors with ICH_3 or nitrogen, the stabilisation energy strongly decreases and becomes repulsive. All of these findings support the charge-transfer character of the mentioned complexes.

iii) The total stabilisation energies correlate well with induction energy including the charge-transfer energy as well as with the $V_{s,max}$ value and the LUMO energy, and the induction energy is the most important attractive term. It should be mentioned again that in all of our previous studies[35-59] on noncovalent complexes including X-bonded complexes, the induction energy was systematically the smallest attractive term.

iv) The halogen bond in the mentioned complexes is thus stabilised mainly by induction (charge-transfer) energy and to a lesser extent by electrostatic energy.

Acknowledgements

This work was part of the Research Project RVO: 61388963 of the Institute of Organic Chemistry and Biochemistry, Academy of Sciences of the Czech Republic. This work was also supported by the Czech Science Foundation [P208/12/G016] and the operational program Research and Development for Innovations of the European Social Fund (CZ 1.05/2.1.00/03/0058).

References

1. J. Rezac, K. E. Riley and P. Hobza, *J. Chem. Theory Comput.*, 2012, **8**, 4285-4292.
2. J. Rezac, K. E. Riley and P. Hobza, *J. Chem. Theory Comput.*, 2011, **7**, 2427-2438.
3. L. F. Molnar, X. He, B. Wang and K. M. Merz Jr, *The J. Chem. Phys.*, 2009, **131**, 065102-06517.
4. T. Clark, M. Hennemann, J. S. Murray and P. Politzer, *J. Mol. Model.*, 2007, **13**, 291-296.
5. P. Politzer, J. S. Murray and T. Clark, *Phys. Chem. Chem. Phys.*, 2013, **15**, 11178-11189.
6. P. Politzer and J. S. Murray, *ChemPhysChem*, 2013, **14**, 278-294.
7. E. Arunan, G. R. Desiraju, R. A. Klein, J. Sadlej, S. Scheiner, I. Alkorta, D. C. Clary, R. H. Crabtree, J. J. Dannenberg, P. Hobza, Henrik G. Kjaergaard, Anthony C. Legon, Benedetta. Mennucci, and D. J. Nesbitt, *Pure Appl. Chem.*, 2011, **83**, 1619-1636.
8. E. Arunan, G. R. Desiraju, R. A. Klein, J. Sadlej, S. Scheiner, I. Alkorta, D. C. Clary, R. H. Crabtree, J. J. Dannenberg, P. Hobza, Henrik G. Kjaergaard, Anthony C. Legon, Benedetta. Mennucci, and D. J. Nesbitt, *Pure Appl. Chem.*, 2011, **83**, 1637-1641.
9. A. Hesselmann and G. Jansen, *Chem. Phys. Lett.*, 2002, **357**, 464-470.
10. A. Hesselmann and G. Jansen, *Chem. Phys. Lett.*, 2002, **362**, 319-325.
11. A. J. Misquitta and K. Szalewicz, *Chem. Phys. Lett.*, 2002, **357**, 301-306.
12. G. Jansen and A. Hesselmann, *J. Phys. Chem. A*, 2001, **105**, 11156-11157.
13. A. Hesselmann and G. Jansen, *Chem. Phys. Lett.*, 2003, **367**, 778-784.
14. A. Hesselmann, G. Jansen and M. Schütz, *The J. Chem. Phys.*, 2005, **122**, 014103-014119.
15. A. Hesselmann, G. Jansen and M. Schütz, *J. Am. Chem. Soc.*, 2006, **128**, 11730-11731.
16. R. Podeszwa, R. Bukowski and K. Szalewicz, *J. Phys. Chem. A*, 2006, **110**, 10345-10354.
17. H. L. Williams and C. F. Chabalowski, *J. Phys. Chem. A*, 2001, **105**, 646-659.
18. P. Deepa, B. V. Pandiyan, P. Kolandaivel and P. Hobza, *Phys. Chem. Chem. Phys.*, 2014, **16**, 2038-2047.
19. A. Peuronen, A. Valkonen, M. Kortelainen, K. Rissanen and M. Lahtinen, *Cryst. Growth Des.*, 2012, **12**, 4157-4169.
20. B. Jeziorski, R. Moszynski and K. Szalewicz, *Chem. Rev.*, 1994, **94**, 1887-1930.
21. R. F. Bader, M. T. Carroll, J. R. Cheeseman and C. Chang, *J. Am. Chem. Soc.*, 1987, **109**, 7968-7979.
22. A. D. Becke, *J. Chem. Phys.*, 1997, **107**, 8554-8560.
23. H. L. Schmider and A. D. Becke, *J. Chem. Phys.*, 1998, **108**, 9624-9631.
24. S. Grimme, S. Ehrlich and L. Goerigk, *J. Comp. Chem.*, 2011, **32**, 1456-1465.
25. A. Halkier, T. Helgaker, P. Jorgensen, W. Klopper and J. Olsen, *Chem. Phys. Lett.*, 1999, **302**, 437-446.
26. A. Halkier, T. Helgaker, P. Jorgensen, W. Klopper, H. Koch, J. Olsen and A. K. Wilson, *Chem. Phys. Lett.*, 1998, **286**, 243-252.
27. S. Kozuch and J. M. Martin, *J. Chem. Theory Comput.*, 2013, **9**, 1918-1931.
28. Y. Zhao and D. G. Truhlar, *Theoretical Chemistry Accounts*, 2008, **120**, 215-241.

29. S. F. Boys and F. Bernardi, *Mol. Phys.*, 1970, 19, 553-557.
30. MOLPRO, version 2010.1, a package of ab initio programs, Werner, H.-J.; Knowles, P. J.; Manby, F. R.; Schuetz, M.; Celani, P.; Knizia, G.; Korona, T.; Lindh, R.; Mitrushenkov, A.; Rauhut, G.; Adler, T. B.; Amos, R. D.; Bernhardsson, A.; Berning, A.; Cooper, D. L.; O. Deegan, M. J.; Dobbyn, A. J.; Eckert, F.; Goll, F.; Hampel, C.; Hesselmann, A.; Hetzer, G.; Hrenar, T.; Jansen, G.;Koeppl, C.; Liu, Y.; Lloyd, A. W.; Mata, R. A.; May, A. J.; McNicholas, S. J.; Meyer, W.; Mura, M. E.; Nicklass, A.; Palmieri, P.; Pflueger, K.; Pitzer, K.; Reiher, M.; Shiozaki, T.; Stoll, H.; Stone, A. J.; Tarroni, R.; Thorsteinsson, T.; Wang, M.; Wolf, A., 2010, see http://www.molpro.net
31. TURBOMOLE V6.3 2011, a development of University of Karlsruhe and Forschungszentrum Karlsruhe GmbH, 1989-2007, TURBOMOLE GmbH, since 2007; available from http://www.turbomole.com.
32. Gaussian 09, *Revision D.01*, Frisch, M. J.; Trucks, G. W.; Schlegel, H. B.; Scuseria, G. E.; Robb, M. A.; Cheeseman, J. R.; Scalmani, G.; Barone, V.; Mennucci, B.; Petersson, G. A.; Nakatsuji, H.; Caricato, M.; Li, X.; Hratchian, H. P.; Izmaylov, A. F.; Bloino, J.; Zheng, G.; Sonnenberg, J. L.; Hada, M.; Ehara, M.; Toyota, K.; Fukuda, R.; Hasegawa, J.; Ishida, M.; Nakajima, T.; Honda, Y.; Kitao, O.; Nakai, H.; Vreven, T.; Montgomery, Jr., J. A.; Peralta, J. E.; Ogliaro, F.; Bearpark, M.; Heyd, J. J.; Brothers, E.; Kudin, K. N.; Staroverov, V. N.; Kobayashi, R.; Normand, J.; Raghavachari, K.; Rendell, A.; Burant, J. C.; Iyengar, S. S.; Tomasi, J.; Cossi, M.; Rega, N.; Millam, N. J.; Klene, M.; Knox, J. E.; Cross, J. B.; Bakken, V.; Adamo, C.; Jaramillo, J.; Gomperts, R.; Stratmann, R. E.; Yazyev, O.; Austin, A. J.; Cammi, R.; Pomelli, C.; Ochterski, J. W.; Martin, R. L.; Morokuma, K.; Zakrzewski, V. G.; Voth, G. A.; Salvador, P.; Dannenberg, J. J.; Dapprich, S.; Daniels, A. D.; Farkas, O.; Foresman, J. B.; Ortiz, J. V.; Cioslowski, J.; Fox, D. J., Gaussian, Inc.: Wallingford, CT, 2009.
33. G. Schaftenaar and J. H. Noordik, "Molden: a pre- and post-processing program for molecular and electronic structures", *J. Comput.-Aided Mod. Des.*, 2000, **14**, 123-134.
34. M. Pitonak, K. E. Riley, P. Neogrady and P. Hobza, *ChemPhysChem*, 2008, **9**, 1636-1644.
35. W. Zierkiewicz, D. Michalska and P. Hobza, *Phys. Chem. Chem. Phys.*, 2010, **12**, 2888-2894.
36. E. Munusamy, R. Sedlak and P. Hobza, *ChemPhysChem*, 2011, **12**, 3253-3261.
37. R. Sedlak, P. Jurecka and P. Hobza, *The J. Chem. Phys.*, 2007, **127**, 075104-075106.
38. J. Rezac and P. Hobza, *J. Chem. Theory Comput.*, 2011, **7**, 685-689.
39. R. Sedlak, J. Fanfrlík, D. Hnyk, P. Hobza and M. Lepsík, *J. Phys. Chem. A*, 2010, **114**, 11304-11311.
40. S. Karthikeyan, R. Sedlak and P. Hobza, *J. Phys. Chem. A*, 2011, **115**, 9422-9428.
41. W. Wang and P. Hobza, *ChemPhysChem*, 2008, **9**, 1003-1009.
42. R. Sedlak, P. Hobza and G. N. Patwari, *J. Phys. Chem. A*, 2009, **113**, 6620-6625.
43. S. Maity, R. Sedlak, P. Hobza and G. N. Patwari, *Phys. Chem. Chem. Phys.*, 2009, **11**, 9738-9743.
44. J. Ran and P. Hobza, *J. Phys. Chem. B*, 2009, **113**, 2933-2936.
45. L. Biedermannova, K. E. Riley, K. Berka, P. Hobza and J. Vondrasek, *Phys. Chem. Chem. Phys.*, 2008, **10**, 6350-6359.
46. M. Kolar, K. Berka, P. Jurecka and P. Hobza, *ChemPhysChem*, 2010, **11**, 2399-2408.
47. C. A. Morgado, P. Jurecka, D. Svozil, P. Hobza and J. Sponer, *Phys. Chem. Chem. Phys.*, 2010, **12**, 3522-3534.
48. J. Cerny and P. Hobza, *Phys. Chem. Chem. Phys.*, 2007, **9**, 5291-5303.

49. K. Berka, P. Hobza and J. Vondrasek, *ChemPhysChem*, 2009, **10**, 543-548.
50. K. E. Riley, M. Pitonak, J. Cerny and P. Hobza, *J. Chem. Theory Comput.*, 2010, **6**, 66-80.
51. K. E. Riley and P. Hobza, *Wiley Interdiscip. Rev. Comput. Mol. Sci.*, 2011, **1**, 3-17.
52. L. Bendova, P. Jurecka, P. Hobza and J. Vondrasek, *J. Phys. Chem. B*, 2007, **111**, 9975-9979.
53. J. Ran and P. Hobza, *J. Chem. Theory Comput.*, 2009, **5**, 1180-1185.
54. S. Maity, G. N. Patwari, R. Sedlak and P. Hobza, *Phys. Chem. Chem. Phys.*, 2011, **13**, 16706-16712.
55. J. Sponer, K. E. Riley and P. Hobza, *Phys. Chem. Chem. Phys.*, 2008, **10**, 2595-2610.
56. M. Zgarbova, M. Otyepka, J. Sponer, P. Hobza and P. Jurecka, *Phys. Chem. Chem. Phys.*, 2010, **12**, 10476-10493.
57. W. Zierkiewicz, R. Wieczorek, P. Hobza and D. Michalska, *Phys. Chem. Chem. Phys.*, 2011, **13**, 5105-5113.
58. K. Pluhackova, P. Jurecka and P. Hobza, *Phys. Chem. Chem. Phys.*, 2007, **9**, 755-760.
59. U. Adhikari and S. Scheiner, *Chem. Phys. Lett.*, 2012, **532**, 31-35.

Fig. 1 Crystal structures of complexes investigated with halogen bond length (Å). Red colour represents iodine, magenta oxygen, blue sulphur, pale yellow nitrogen, orange carbon and white hydrogen.

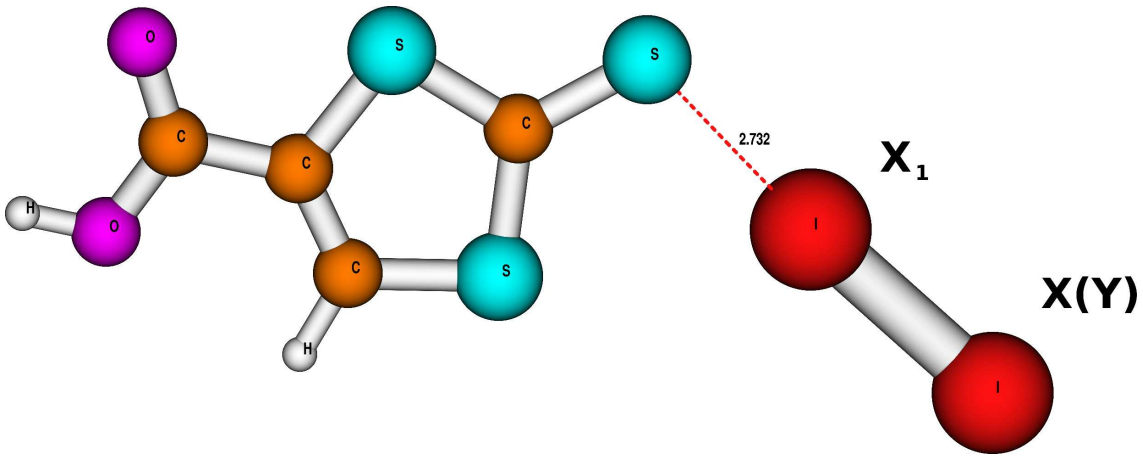

a) DTCA...I_2 complex

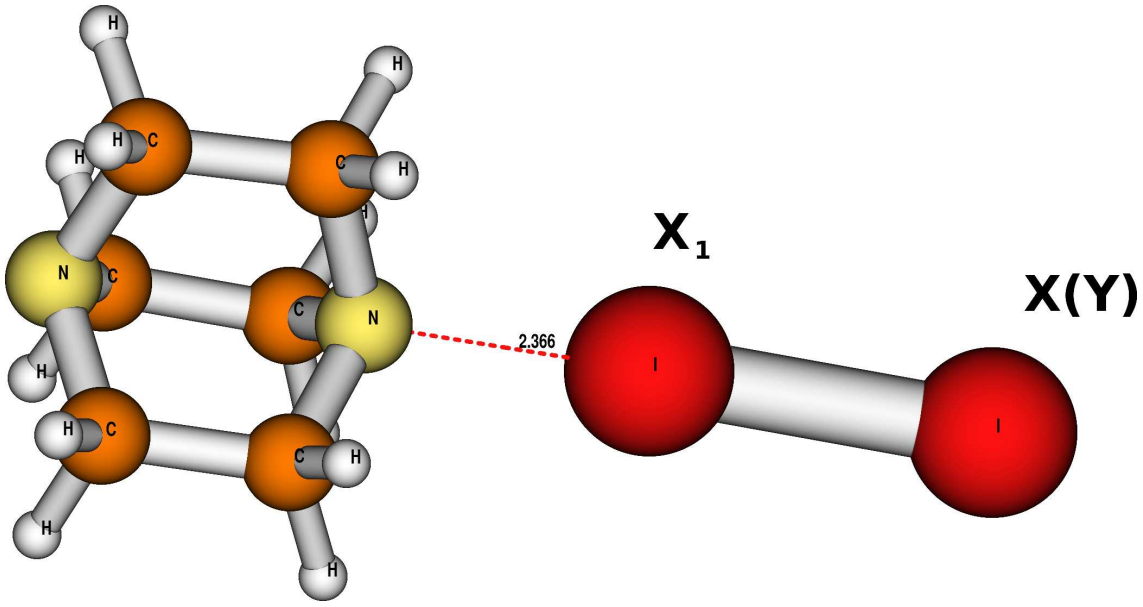

b) DABCO... I_2 complex

Fig. 2 Electrostatic potential (a.u.) for all the monomers: I_2, Br_2, Cl_2, N_2, IF and ICH_3. Here blue and red colour indicates positive and negative region, respectively.

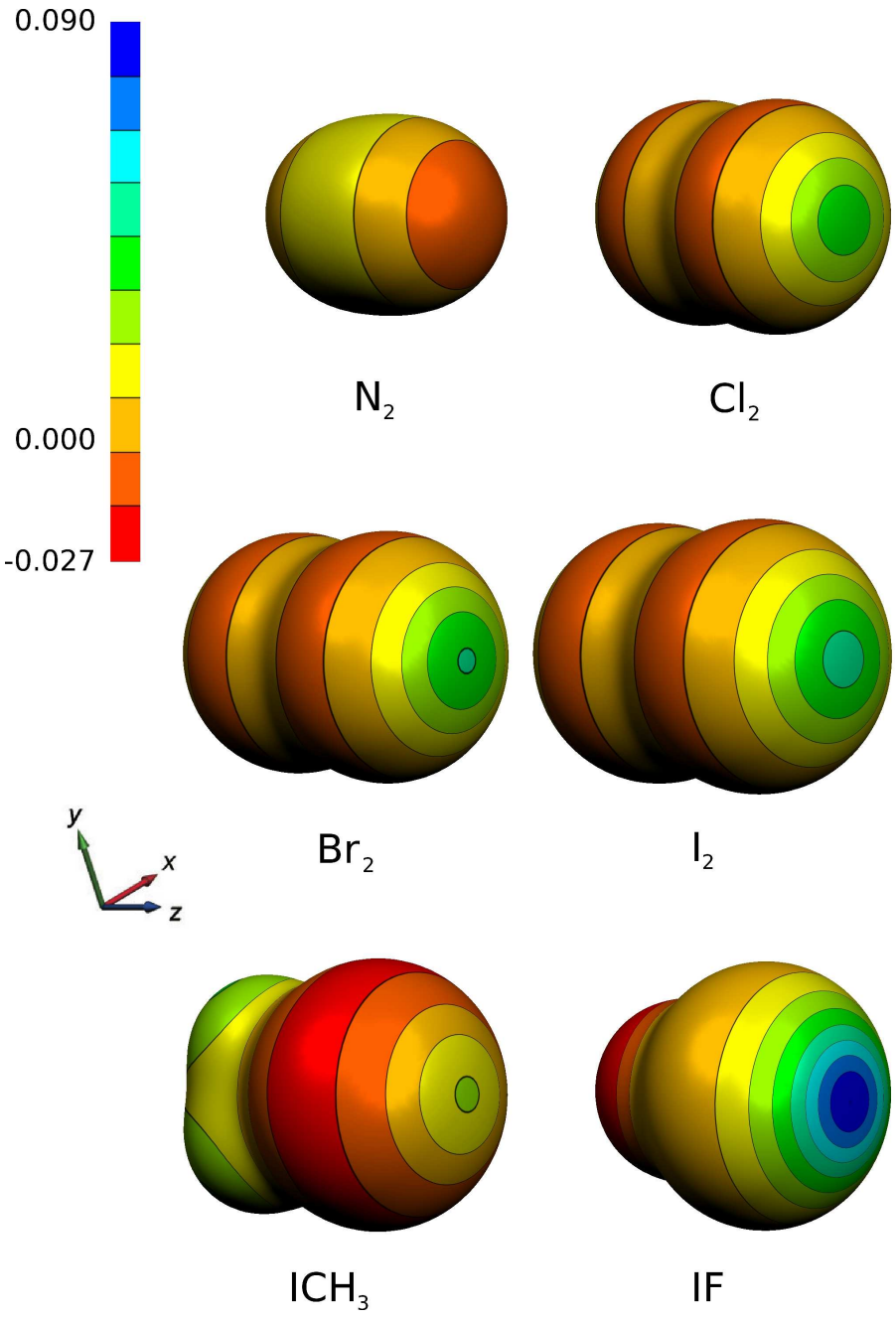

Fig. 3a Correlation between QM and $V_{s,max}$ for I_2, Br_2, Cl_2, N_2 molecules (In all subsequent plots of Figure 3 QM stands for quadrupole moment and following units are used: [Vs,max] = a.u., [QM] = a.u. and all interaction energy values are listed in kcal/mol).

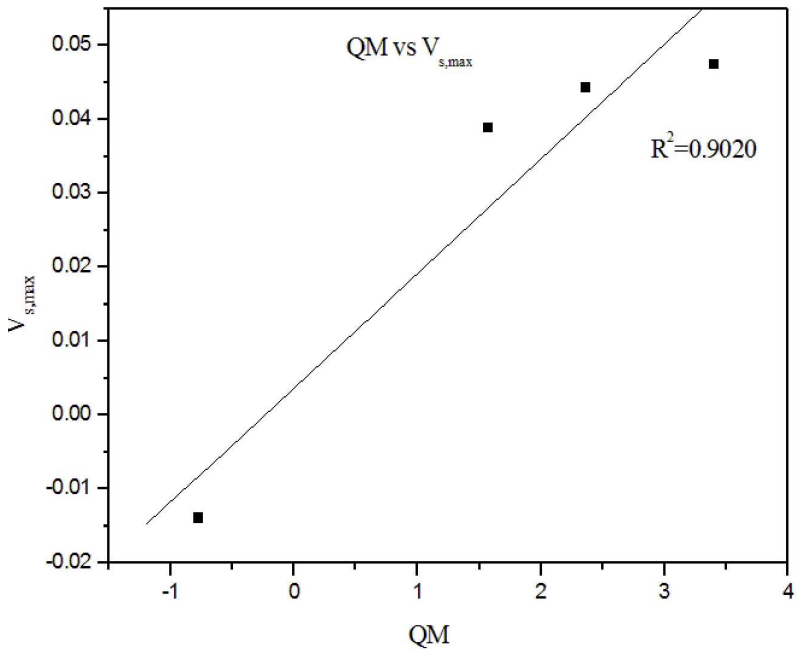

Fig. 3b Correlation between M062X and CCSD(T)/CBS interaction energies for DTCA (left) and DABCO (right) set of complexes.

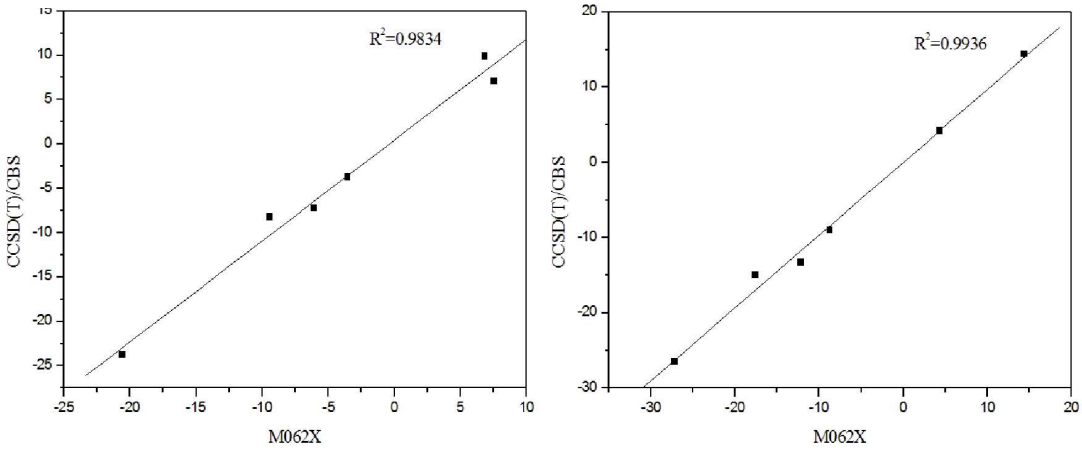

DTCA **DABCO**

Fig. 3c Correlation between CCSD(T)/CBS and DFT-SAPT interaction energies for DTCA (left) and DABCO (right) set of complexes.

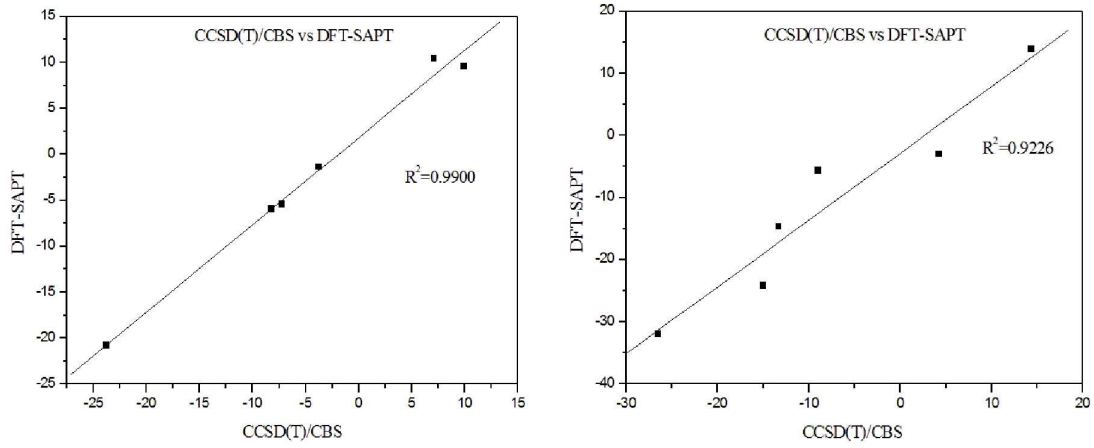

DTCA **DABCO**

Fig. 3d Correlation between $V_{s,\,max}$ and E_1^{Pol} (left); QM and E_1^{Pol} (right) for I_2, Br_2, Cl_2, N_2…DTCA complexes.

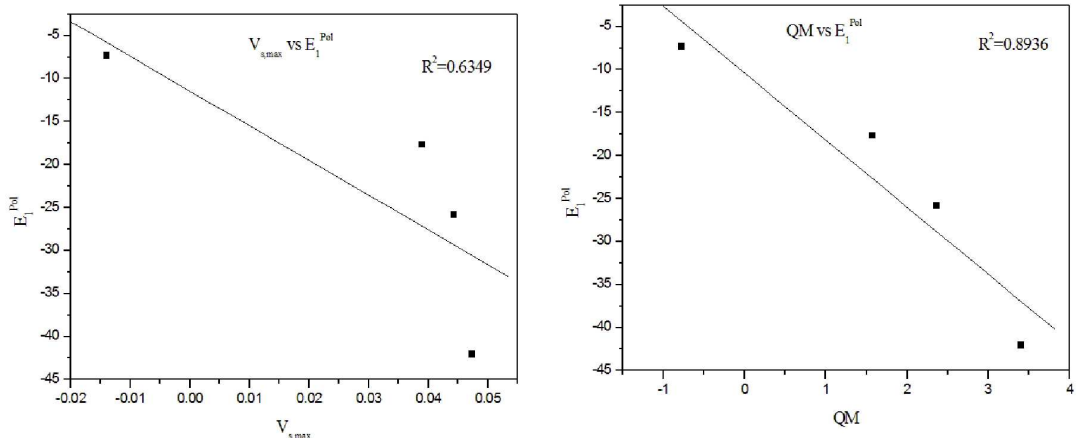

Fig. 3e Correlation between $V_{s,\,max}$ and E_1^{Pol} (left); QM and E_1^{Pol} (right) for I_2, Br_2, Cl_2, N_2…DABCO complexes.

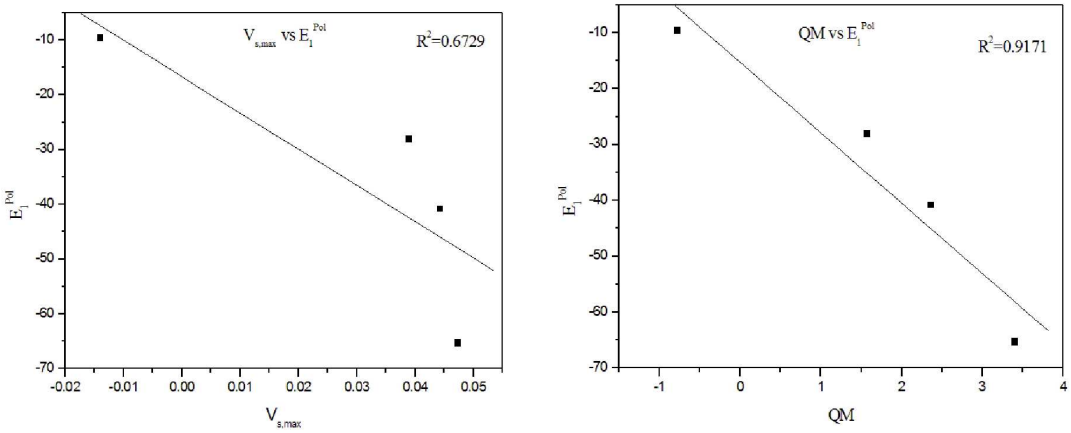

Fig. 3f Correlation between $V_{s,\,max}$ and E_1^{Pol} for DTCA (left) and DABCO (right) set of complexes.

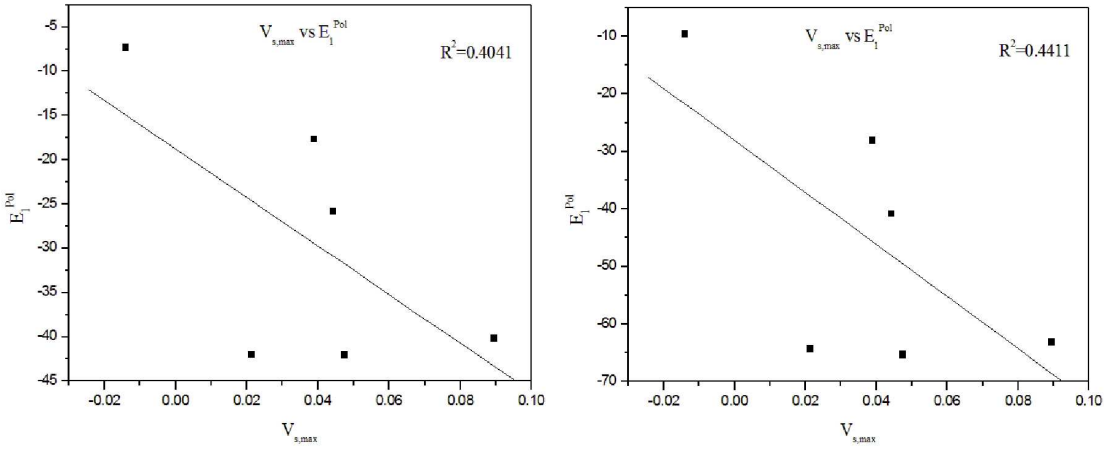

DTCA **DABCO**

Fig. 3g Correlation between $V_{s,max}$ and E_2^{Ind} for DTCA (left) and DABCO (right) set of complexes.

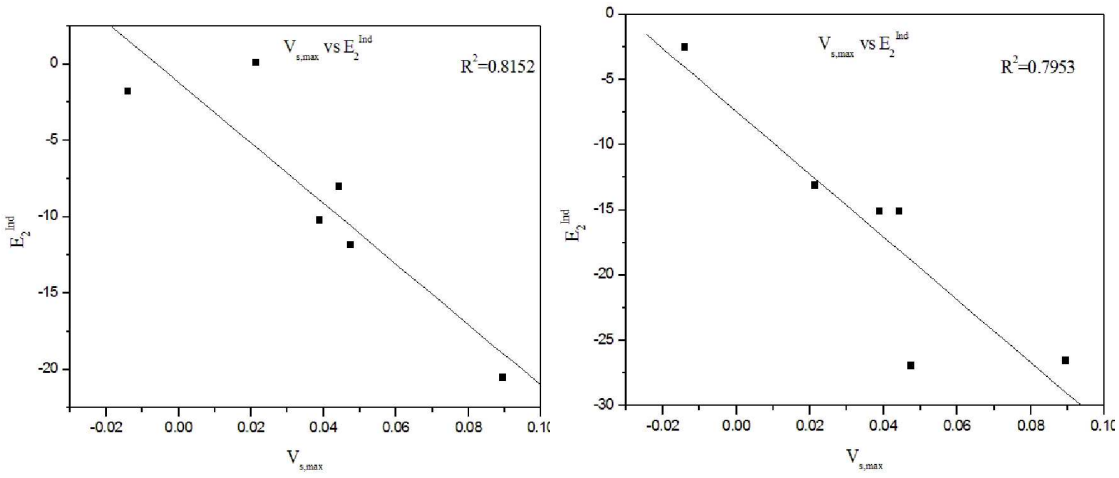

DTCA **DABCO**

Fig. 3h Correlation between LUMO and E_2^{Ind} for DTCA (left) and DABCO (right) set of complexes.

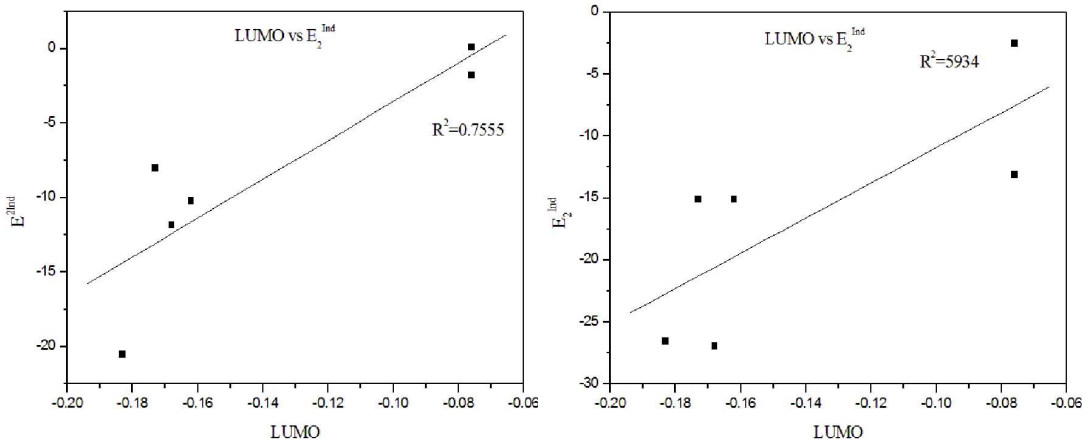

DTCA **DABCO**

Fig. 3i Correlation between $V_{s,max}$ and DFT-SAPT for DTCA (left) and DABCO (right) set of complexes.

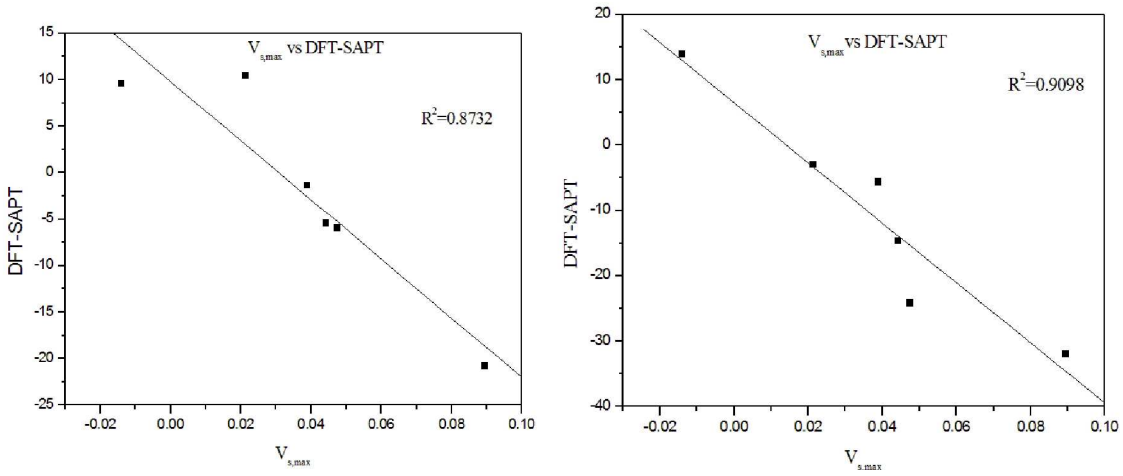

DTCA **DABCO**

Fig. 3j Correlation between $V_{s,max}$ and CCSD(T)/CBS for DTCA (left) and DABCO (right) set of complexes.

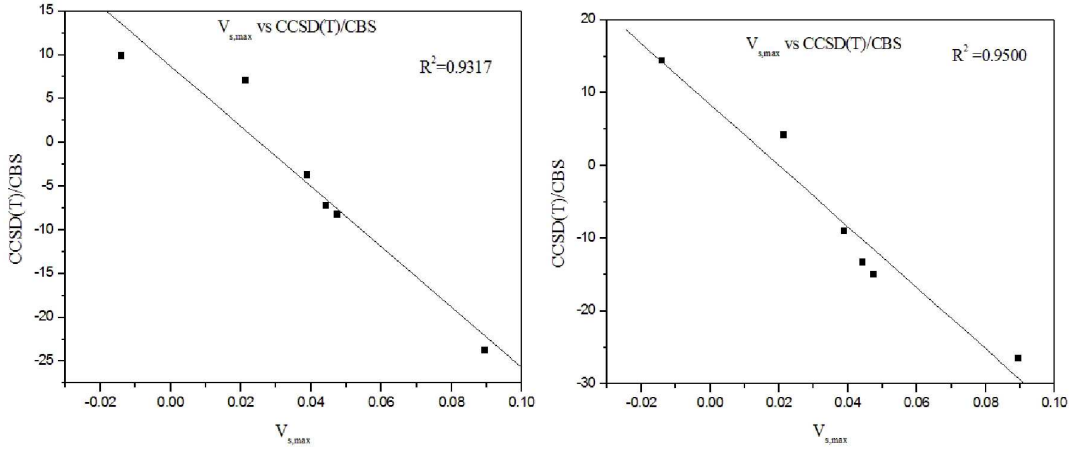

DTCA **DABCO**

Fig. 3k Correlation between LUMO and DFT-SAPT for DTCA (left) and DABCO (right) set of complexes.

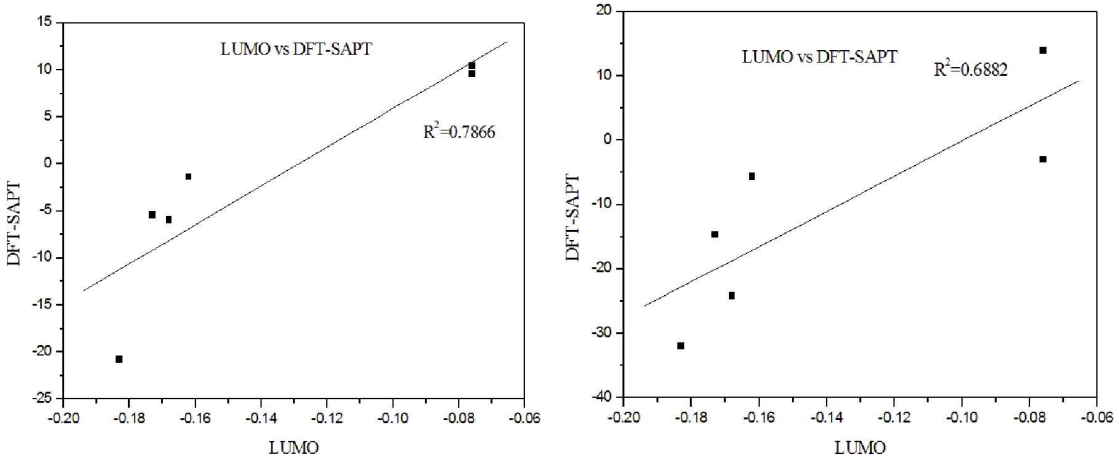

DTCA **DABCO**

Fig. 3l Correlation between LUMO and CCSD(T)/CBS for DTCA (left) and DABCO (right) set of complexes.

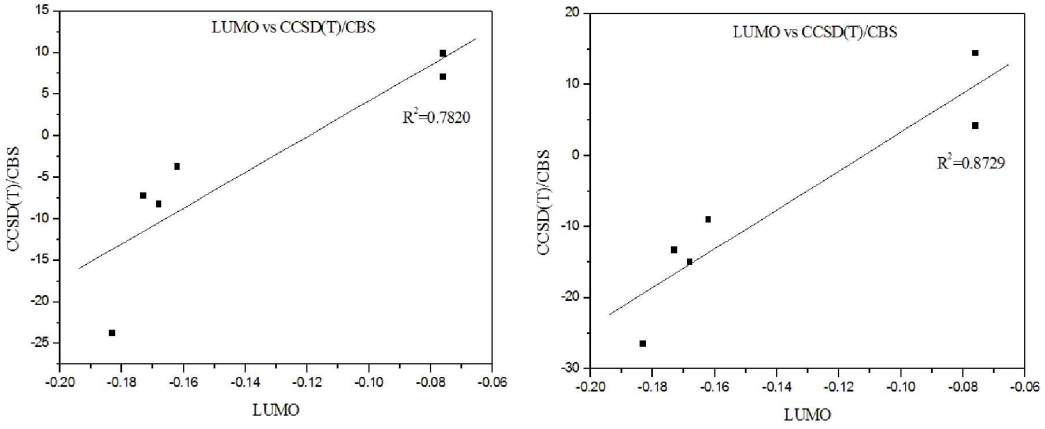

DTCA **DABCO**

Fig. 3m Correlation between DFT-SAPT and E_2^{Ind} for DTCA (left) and DABCO (right) set of complexes.

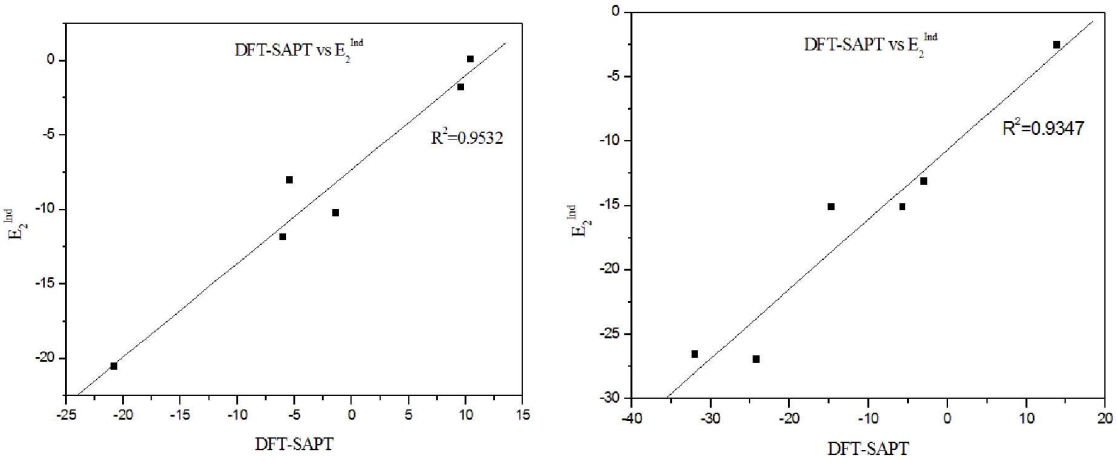

DTCA **DABCO**

Table 1 The Q_{zz} component of the quadrupole moment (a.u.), LUMO (a.u.) and $V_{s,max}$ at 0.001 a.u. isodensity surface for selected monomers calculated at the B97-D3/def2-QZVP level of theory. $V_{s,max}$ value corresponds to the cusp/pick point of the halogen atom.

	Quadruple moment	LUMO	$V_{s,max}$
I_2	3.402	-0.168	0.0474
Br_2	2.362	-0.173	0.0443
Cl_2	1.574	-0.162	0.0389
N_2	-0.774	-0.076	-0.0140
IF	0.273	-0.183	0.0896
ICH_3	3.217	-0.076	0.0214

Table 2 The stabilization energies (-E_{int}; in kcal/mol) calculated at the DFT-D (B97-D3/def2-QZVP), M062X/def2-QZVP, CCSD(T)/CBS and DFT-SAPT/aug-cc-pVDZ levels of theory. In all of the cases, the intermolecular distances X...S and X...N contacts amount to 2.73Å and 2.37Å, respectively. The numbers in the round brackets correspond to dispersion energy (in kcal/mol).

SYSTEMS	B97-D3/ def2-QZVP	M062X/ def2-QZVP	CCSDT/ CBS	DFT-SAPT/ aug-cc-pVDZ	MP2/ CBS
DTCA...I_2	13.80 (-5.38)	8.81	8.20	5.98	12.36
DTCA ...Br_2	11.25 (-4.45)	6.97	7.21	5.42	10.27
DTCA ...Cl_2	8.34 (-3.82)	3.40	3.75	1.36	6.01
DTCA ...N_2	-10.11 (-2.61)	-10.03	-9.93	-9.57	-9.11
DTCA ...IF	29.27 (-5.01)	25.10	23.77	20.81	27.21
DTCA ...ICH_3	-4.33 (-5.20)	-8.12	-7.08	-10.43	-3.98
DABCO...I_2	18.97 (-8.33)	17.18	15.01	24.19	20.31
DABCO...Br_2	16.72 (-6.58)	13.04	13.31	14.68	17.21
DABCO...Cl_2	13.79 (-5.39)	8.47	8.98	5.68	11.72
DABCO...N_2	-14.55 (-3.44)	-14.40	-14.40	-13.92	-14.02
DABCO...IF	28.22 (-8.03)	26.94	26.49	31.98	30.29
DABCO...ICH_3	-2.69 (-8.19)	-4.90	-4.21	-3.01	-0.89

Table 3 The DFT-SAPT/aug-cc-pVDZ interaction energies (in kcal/mol). For exact definition of particular terms c.f. subsection Calculations.

complex/term	E_{tot}	E_1^{Pol}	E_1^{Ex}	$E_2^{ind}+E_2^{ex-ind}$	E_2^{Disp}	δHF	E_2^{Ind}
DTCA acid...I2	-5.98	-42.06	59.00	-67.07	-11.11	55.25	-11.82
DTCA...Br2	-5.42	-25.82	36.97	-22.09	-8.54	14.05	-8.03
DTCA...Cl2	-1.36	-17.68	33.34	-4.37	-6.79	-5.86	-10.23
DTCA...N2	9.57	-7.28	23.01	-0.33	-4.39	-1.45	-1.78
DTCA...IF	-20.81	-40.19	49.97	-66.41	-10.05	45.86	-20.55
DTCA...ICH3	10.43	-42.01	63.60	-66.01	-11.25	66.10	0.09
DABCO...I2	-24.19	-65.36	83.02	-93.51	-14.91	66.57	-26.94
DABCO...Br2	-14.68	-40.81	52.52	-31.82	-11.29	16.73	-15.09
DABCO...Cl2	-5.68	-28.10	46.47	-7.20	-8.95	-7.91	-15.11
DABCO...N2	13.92	-9.65	31.82	-0.71	-5.71	-1.82	-2.54
DABCO...IF	-31.98	-63.24	71.35	-90.82	-13.55	64.28	-26.54
DABCO...ICH3	-3.01	-64.32	89.58	-92.07	-15.17	78.97	-13.10